Available online at www.sciencedirect.com
SCIENCE DIRECT®
Global and Planetary Change 38 (2003) 191–208
GLOBAL AND PLANETARY CHANGE
www.elsevier.com/locate/gloplacha

The versatile integrator of surface atmospheric processes Part 2: evaluation of three topography-based runoff schemes

Guo-Yue Niu, Zong-Liang Yang*

Department of Geological Sciences, The University of Texas at Austin, Austin, TX 78712-1101, USA

Received 30 November 2001; received in revised form 4 February 2002; accepted 31 May 2002

Abstract

Three different schemes of topography-based runoff production [versatile integrator of surface atmospheric processes (VISA)-TOP1, VISA-TOP2, and VISA-TOP3] are described for a land-surface model (LSM) developed for use with a general circulation model (GCM). The schemes' sensitivities to some key parameters are assessed for two catchments using data sets developed for the Project for Intercomparison of Land-Surface Parameterization Schemes (PILPS) Phase 2e. VISA-TOP1 differs from VISA-TOP2 only in how to treat oversaturated soil water from the soil layers. In VISA-TOP1, the oversaturated soil water is thrown out of the soil column; hence, it no longer plays a role in the ensuing soil water budgets. In VISA-TOP2, this oversaturated soil water is recharged back to the unsaturated soil layers above the water table; hence, it continues to involve in the water budgets. Unlike VISA-TOP1 and VISA-TOP2, VISA-TOP3 relaxes its dependence on the topographic parameters. The oversaturated soil water is treated the same in both VISA-TOP2 and VISA-TOP3. All three models reproduce the daily and seasonal cycles of streamflow provided that different values of the saturated hydraulic conductivity decay factor are used. The decay factor controls the timing and partitioning of subsurface runoff. In both VISA-TOP1 and VISA-TOP2, an anisotropic parameter explaining different hydraulic conductivities in the vertical and horizontal directions is critical for using the topographic index in the land-surface model. In the VISA-TOP2 scheme, the topography-controlled subsurface runoff is dominant because the oversaturated water is recharged to upper unsaturated soil layers to raise the water table. The water budgets in all these schemes show dramatically different responses to the decay factor, indicating that the calibrated parameters and the model formulations should not be separated.

Keywords: VISA-TOP1; VISA-TOP2; VISA-TOP3

1. Introduction

Parameterization of runoff-related processes in soil vegetation–atmosphere transfer (SVAT) schemes has been an active research topic. There is an increasing awareness that the parameterization needs to explicitly account for the topographic control on the soil moisture distribution and the runoff production.

Beven and Kirkby (1979) were among the first to develop a simple conceptual model at the hillslope and the catchment scales to model the runoff production using information on hillslope topography and

* Corresponding author. Tel.: +1-512-471-3824; fax: +1-512-471-9425.
E-mail address: liang@mail.utexas.edu (Z.-L. Yang).

0921-8181/03/$ - see front matter © 2003 Elsevier Science B.V. All rights reserved.
doi:10.1016/S0921-8181(03)00029-8

soil and rainfall variabilities. The so-called TOPography-based hydrological MODEL (TOPMODEL) formalism has undergone significant enhancements over the years (Beven and Kirkby, 1979; Beven et al., 1994, 1995). Recently, the basic TOPMODEL approach has been employed by various SVAT schemes developed for use with general circulation models (GCMs) (Famiglietti and Wood, 1991; Stieglitz et al., 1997; Koster et al., 2000; Ducharne et al., 2000; Chen and Kumar, 2001). Yang et al. (2000) implemented a topography-based runoff scheme into the common land model (CLM) (Dai et al., 2003), and the resulting model was tested with the meteorological and streamflow data from the Red-Arkansas River basins.

It is well recognized that TOPMODEL involves a considerable amount of uncertainties due to its basic assumptions, meaning of the model parameters, and derivation of topographic index distributions from digital terrain data at different resolutions (Beven, 1997). However, it is still attractive for climate modelers to use the TOPMODEL concept to parameterize the topographic effects in SVATs for climate studies. Such parameterization may involve three steps: (1) implementing the TOPMODEL concept in a SVAT model, testing alternative formulations, and determining sensitive parameters in offline mode at the hillslope and catchment scales; (2) testing model formulations and determining parameters in offline mode on a global basis; and (3) testing model formulations, determining parameters, and studying the surface water–climate interaction with GCMs. This paper addresses the first step.

Yang and Niu (2003-this issue), hereafter referred to as Paper 1, describes an integration of recent advances in snow physics, topography-related runoff processes, and leaf growth into the National Center for Atmospheric Research (NCAR) Land-Surface Model (LSM) of Bonan (1996). The resulting model is called the versatile integrator of the surface atmospheric (VISA) processes. In the present paper, we describe three parameterization schemes of topography-related runoff in VISA. The schemes' sensitivities to some key parameters are assessed for two catchments using data sets developed for the Project for Intercomparison of Land-Surface Parameterization Schemes (PILPS) Phase 2e (Bowling et al., 2003-this issue).

2. Parameterization of topographic effects on runoff production: VISA-TOP1

While Paper 1 has detailed a topography-related parameterization scheme of runoff in VISA, this section describes a variant of the runoff scheme, hereafter referred to as VISA-TOP1. In order to focus on the topographic effects, the VISA model in this paper does not include the leaf growth component described in Paper 1.

2.1. Saturated hydraulic conductivity

The saturated hydraulic conductivity decreases exponentially with depth according to

$$K_{\mathrm{sat}}(z) = K_{\mathrm{sat}}(0)e^{-fz} \quad (1)$$

where $K_{\mathrm{sat}}(0)$ is the surface value of saturated hydraulic conductivity, and $1/f$, the e-folding depth of K_{sat}, can be determined through sensitivity analysis or calibration against the recession curve of the observed streamflow. Table 1 lists values of f used in the literature.

2.2. Surface runoff

Surface runoff consists of overland flow by the Dunne mechanism which requires rainfall to impinge on a saturated ground surface and overland flow by the Horton mechanism which is generated when rainfall rate exceeds the infiltration capacity of the soil. The mathematical representation of the above processes takes in the form of

$$R_{\mathrm{s}} = F_{\mathrm{sat}}Q_{\mathrm{wat}} + (1 - F_{\mathrm{sat}})\max(0, (Q_{\mathrm{wat}} - I_{\mathrm{max}})) \quad (2)$$

where Q_{wat} is the recharging rate at the soil surface, I_{max} is the soil infiltration capacity dependent on soil

Table 1
The values of exponential decay factor, f, of the saturated hydraulic conductivity

Authors	Sites/regions	f
Beven, 1982	Various sites	−2.35–9.15
Famiglietti et al., 1992	FIFE	1.5–5.17
Stieglitz et al., 1997	Sleepers River	3.26
Dai et al., 2002	Global	2.0
Chen and Kumar, 2001	North America	1.8
Yang et al., 2000	Red Arkansas River	8.0

texture and moisture conditions (Entekhabi and Eagleson, 1989), and F_{sat} is the saturated fraction, which is determined by the topographic characteristics and soil moisture state of a grid cell,

$$F_{sat} = \int_{\lambda \geq (\bar{\lambda} + f z_\nabla)} \mathrm{pdf}(\lambda) \mathrm{d}\lambda \tag{3}$$

where $\lambda = \ln(a/\tan\beta)$ is the topographic index where a is the contribution area and $\tan\beta$ is the local slope; $\bar{\lambda}$ is the mean value of λ in the grid cell; pdf(λ) is the probability density function of λ; and z_∇ is the grid-mean water table depth.

2.3. Subsurface runoff

Subsurface runoff is parameterized as,

$$R_{sb} = R_{sb,TOP} + R_{sb,BOT} + R_{sb,SAT} \tag{4}$$

where $R_{sb,TOP}$, $R_{sb,BOT}$, and $R_{sb,SAT}$ represent productions of subsurface runoff due to topographic control, bottom drainage, and saturation excess, respectively.

2.3.1. Topographic control

Following Sivapalan et al. (1987), the production of subsurface runoff due to topographic control is

$$R_{sb,TOP} = \alpha \frac{K_{sat}(0)}{f} e^{-\bar{\lambda}} e^{-f z_\nabla} \tag{5}$$

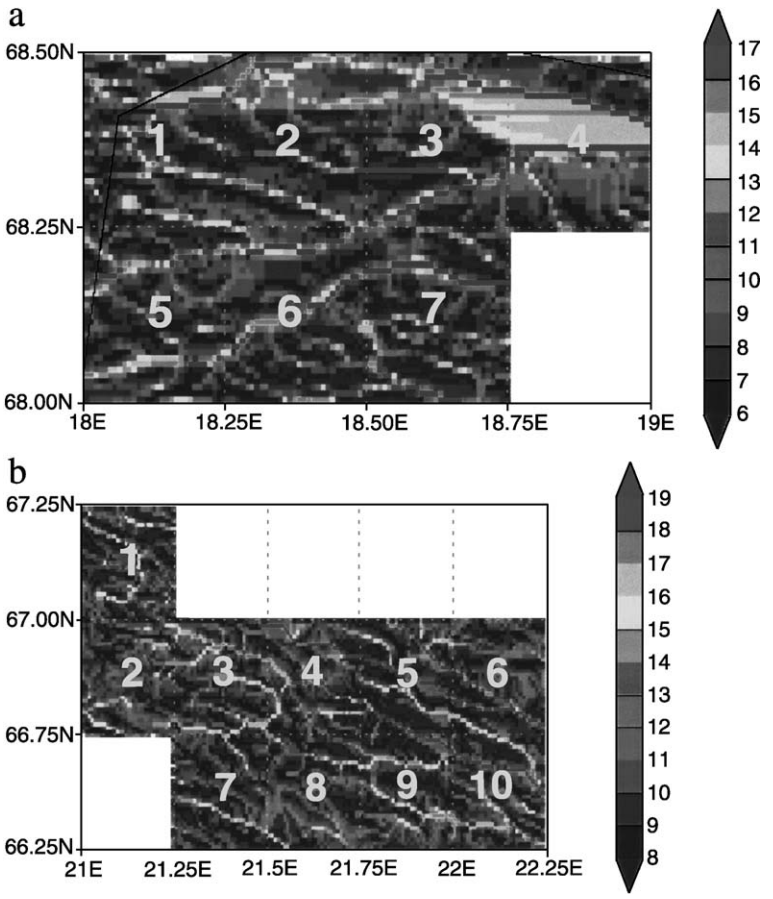

Fig. 1. (a) The topographic index computed from 1000 m DEMs and adjusted according to Eq. (8) for Övre Abiskojokk (seven grid cells). (b) The topographic index computed from 1000 m DEMs and adjusted according to Eq. (8) for Övre Lansjärv (10 grid cells).

where α is an anisotropic factor accounting for the differences in the saturated hydraulic conductivities in the lateral and vertical directions introduced by Chen and Kumar (2001) to simulate the desired streamflow response.

2.3.2. Bottom drainage

The gravitational loss of soil water from the bottom of the model soil column is given by

$$R_{\mathrm{sb,BOT}} = k_6 + \left(\theta_6^{N+1} - \theta_6^{N}\right)\left(\frac{\partial k}{\partial \theta}\right)_6 \quad (6)$$

where k_6 is the hydraulic conductivity at the bottom of the sixth (i.e., the lowest) soil layer, and θ_6^N is the volumetric soil moisture within the sixth soil layer at time step, N.

2.3.3. Saturation excess

The production of subsurface runoff due to saturation excess is

$$R_{\mathrm{sb,SAT}} = \sum_{i=1}^{6} \max[0, ((\theta_i - \theta_{\mathrm{sat}})\Delta z_i/\Delta t)] \quad (7)$$

where θ_i and θ_{sat} are the volumetric soil moisture of the ith layer and the soil porosity, respectively; and Δz_i and Δt are the soil thickness of the ith layer and the timestep, respectively.

2.4. Water table depth

The water table depth, z_∇, is computed following Chen and Kumar (2001). See Paper 1 for details.

3. The topographic index: calculation, distribution and fitting

The topographic index, λ, is often computed from regularly spaced grids of elevation values called digital elevation models (DEMs). While the U.S. Geological Survey (USGS) provides 30-m resolution DEMs for many parts of the USA and about 100 m DEMs for the entire USA, only 1000 m DEMs are available for the entire Earth. It is widely recognized that the distribution of the topographic index is strongly dependent upon the DEM resolution. Wolock and McCabe (2000) proposed a regression equation to relate at 1000-m resolution to that at 100-m resolution as follows:

$$\lambda_{100\ \mathrm{m}} = 0.961 \times \lambda_{1000\ \mathrm{m}} - 1.957 \quad (8)$$

We computed the topographic index in the Swedish Torne–Kalix basin (Bowling et al., 2003-this issue) based on the 1000 m DEM. The values were adjusted according to Eq. (8), and the results for two subbasins, the 566 km^2 Övre Abiskojokk and the 1341 km^2 Övre Lansjärv, are shown in Fig. 1. High values of topographic index are seen near the river channels and lakes (e.g., Grid Cell 4 of Övre Abiskojokk). The topographic parameters, i.e., mean, minimum, maximum, variance, and skewness of the topographic index in each grid cell, are listed in Table 1 for Övre Lansjärv and in Table 2 for Övre Abiskojokk. Following Sivapalan et al. (1987), a three-parameter gamma distribution function was used to fit the actual discrete distribution of the topographic index in each grid cell.

Fig. 2 compares cumulative distribution function (CDF) derived from the analytical three-parameter gamma distribution and from the actual discrete distribution. Basically, the gamma distribution captures the actual distribution for each grid cell especially when λ is greater than $\bar{\lambda}$. Actually, for the calculation of the saturated fraction using Eq. (3), it is not necessary to capture the distribution when λ is less than $\bar{\lambda}$. The maximum saturated fraction (when the mean water table depth is zero) is only determined by the topographic indices. For instance, $\bar{\lambda}$ for Grid 7 in Övre Lansjärv (9.84) corresponds to the CDF value of 38% which is

Table 2
Statistics of the topographic index in Övre Lansjärv

Grid no.	f	Mean	Min.	Max.	Variance	Skewness
1	3.64	10.53	7.11	19.88	7.73	43.47
2	3.55	10.65	7.10	16.44	3.74	24.33
3	3.85	10.80	7.37	19.65	5.74	35.83
4	4.12	10.96	6.70	20.04	8.64	40.17
5	4.23	10.55	6.72	20.09	11.21	43.99
6	4.19	10.45	6.80	20.58	7.55	56.94
7	3.51	9.84	7.17	17.06	3.44	41.96
8	3.73	10.21	7.06	17.47	4.10	26.90
9	4.08	10.32	6.79	19.25	6.09	40.54
10	4.39	10.56	6.70	19.64	8.51	40.16
Average	3.93	10.49	6.95	19.01	6.68	39.43

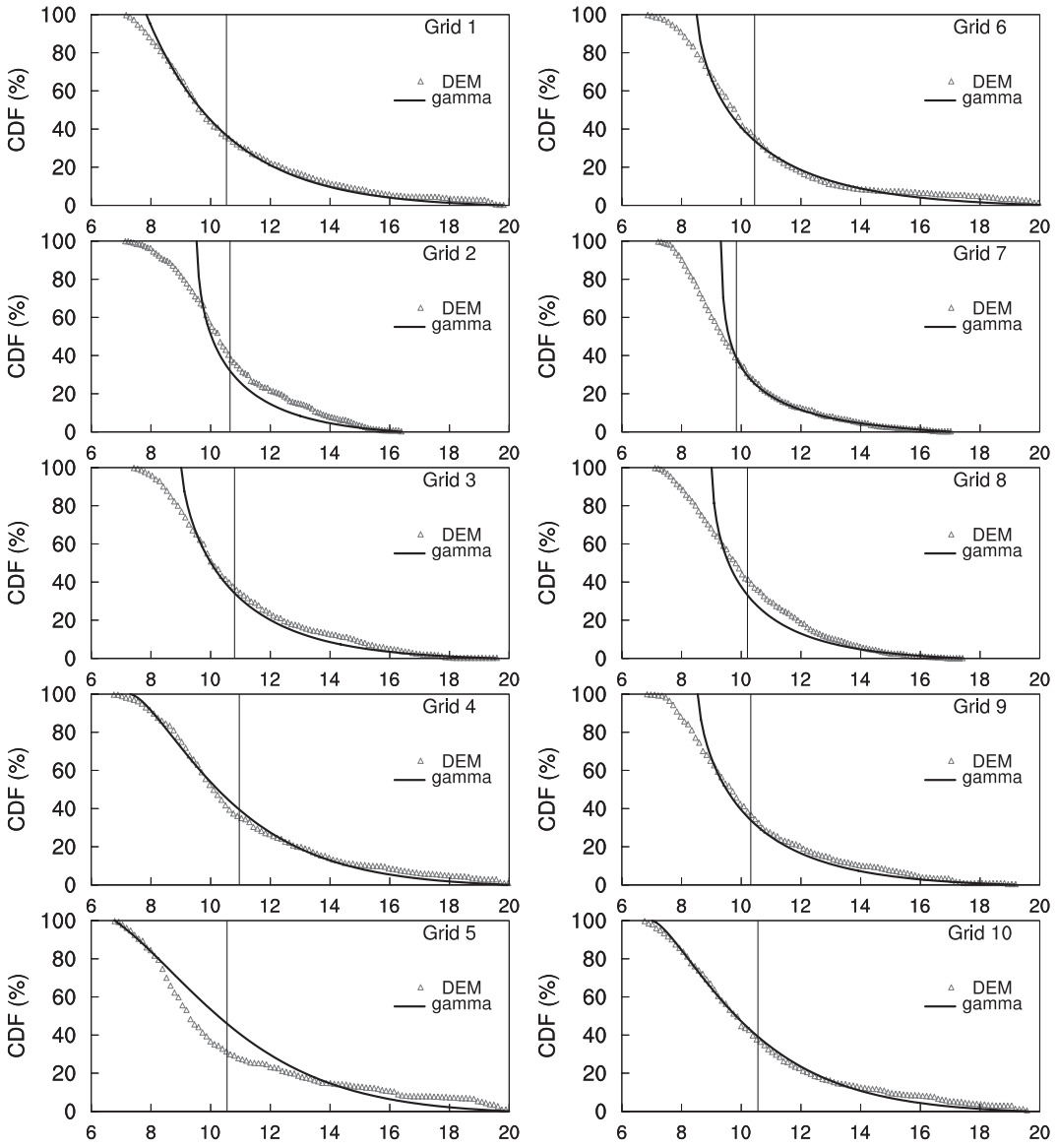

Fig. 2. The cumulative distribution function (CDF) derived from the analytical three-parameter gamma distribution of the topographic index (solid lines) compared with that computed directly from the discrete distribution (triangles) for the 10 grid cells in Övre Lansjärv. The vertical solid line is the mean value of the topographic index.

the maximum saturated fraction when z_{∇} is zero. As z_{∇} increases, the cumulative area for the topographic index greater than $\bar{\lambda}+fz_{\nabla}$ decreases; hence, the saturated fraction is less than its maximum value. The analytical three-parameter gamma distribution is used in the model to improve the computational efficiency.

4. Model demonstration

4.1. Meteorological variables and land-surface characteristics

The data set used in this study is a long-term (1979–1998) hydrometeorological data collected over

the Torne–Kalix River system in Northern Scandinavia, which has a combined area of 58,000 km^2 represented by 218 0.25° computational grid cells at hourly time step. The meteorological forcing data and the land-surface characteristics were described in detail in Bowling et al. (2002). Nine vegetation types provided in the PILPS 2e experimental instructions were combined to form six land-surface types, each consisting of up to four tiles per grid cell (Table 4). Out of the 218 grids in the entire Torne–Kalix river basin, there are 33 grid cells of surface type 1 which was mainly distributed in the mountainous regions, 150 grid cells of surface type 2 in the plain regions, and 31 grids of surface type 3 in the mountain-plain transitional regions. The fractional coverage of vegetation types in each grid cell was taken from the PILPS 2e instructions. The values of other vegetation parameters, such as vegetation height, displacement height, roughness length, architectural resistance, root distribution, and monthly leaf area index, were specified following the PILPS 2e instructions. The minimum stomatal resistance, $r_{s\,\min}$, given in the instructions was converted to the maximum stomatal conductance, $V_{\max}$, using a formula: $V_{\max}=3\rho_a/(c_f r_{s\,\min})$ (Dickinson et al., 1998), where ρ_a is air density and c_f is a conversion factor (7.46×10^{-4} g μmol). Thus, a value of 120.0 m s^{-1} for $r_{s\,\min}$ is approximately equal to 39.3 μmol m^{-2} s^{-1} for $V_{\max}$.

The soil thermal and hydraulic parameters, such as heat capacity, thermal conductivity, hydraulic conductivity, and matrix potential at saturation, b parameter (Clapp and Hornberger, 1978), and porosity, were calculated from percent sand and percent clay using the formulas given in Bonan (1996).

The statistics of the topographic index are given in Tables 2 and 3. Because the saturated hydraulic conductivity decay factor, f, is a calibration parameter, we seek a simple formula relating f calibrated against the observed streamflow for two small catchments to the entire Torne–Kalix basin through use of elevation,

$$f = \max(0.1, a - bz_{\text{top}}) \tag{9}$$

where a and b are two adjustable coefficients, here, $a=5.0$, $b=0.004$; and z_{top} is the grid cell mean elevation in meter. The catchment-averaged decay factor is 3.93 for Övre Lansjärv and 1.36 for Övre Abiskojokk, suggesting that the soil in the lowly lying Övre Lansjärv catchment is more densely compacted than that in the mountainous Övre Abiskojokk catchment.

Table 3
Statistics of the topographic index in Övre Abiskojokk

Grid no.	f	Mean	Min.	Max.	Variance	Skewness
1	1.59	8.84	5.20	17.39	7.22	39.47
2	1.56	8.97	5.25	18.23	7.78	36.25
3	2.21	9.62	5.23	18.77	11.12	30.45
4	2.47	10.70	5.63	18.71	12.79	17.11
5	0.66	8.71	5.63	16.83	6.44	42.85
6	0.61	8.63	4.93	17.85	8.52	47.92
7	0.40	8.59	5.13	18.12	9.55	47.96
Average	1.36	9.15	5.28	17.99	9.06	37.43

4.2. Numerical results

The model was integrated for 11 years from 1988 to1998, and the last 10 years from 1989 to1998 were analyzed for two catchments. Because the catchments span multiple 0.25° grid cells, the modeled runoff from the contributing grid cells was summed and scaled according to the contributing area of each cell. Fig. 3 compares the 10-year time series of the modeled runoff with the observed streamflow. With the parameters specified in Tables 2–4, VISA-TOP1 produces good simulations of streamflow. The surface runoff is dominant in the beginning of the snow-melting season, while the subsurface runoff is dominant during the recession period.

During the melting or raining period, the soil becomes wet, the water table rises, and the saturated fraction is large (Fig. 4); hence, surface runoff is large. Although Övre Lansjärv has a shallower water table, its saturated fraction is lower than that in Övre Abiskojokk because the former has a larger f and a smaller fraction of lakes. The saturated fraction in Övre Abiskojokk varies from 20% to 32%, compared to that from 10% to 22% in Övre Lansjärv.

Not only is the hydrograph different in both catchments, the proportions of subsurface runoff also show distinct patterns. In Övre Lansjärv, $R_{\text{sb,BOT}}$ is zero, whereas it is most pronounced in Övre Abiskojokk. $R_{\text{sb,SAT}}$ is dominant in Övre Lansjärv, while it is relatively modest in Övre Abiskojokk. $R_{\text{sb,TOP}}$ is weak in both catchments, especially in the lower Övre Lansjärv.

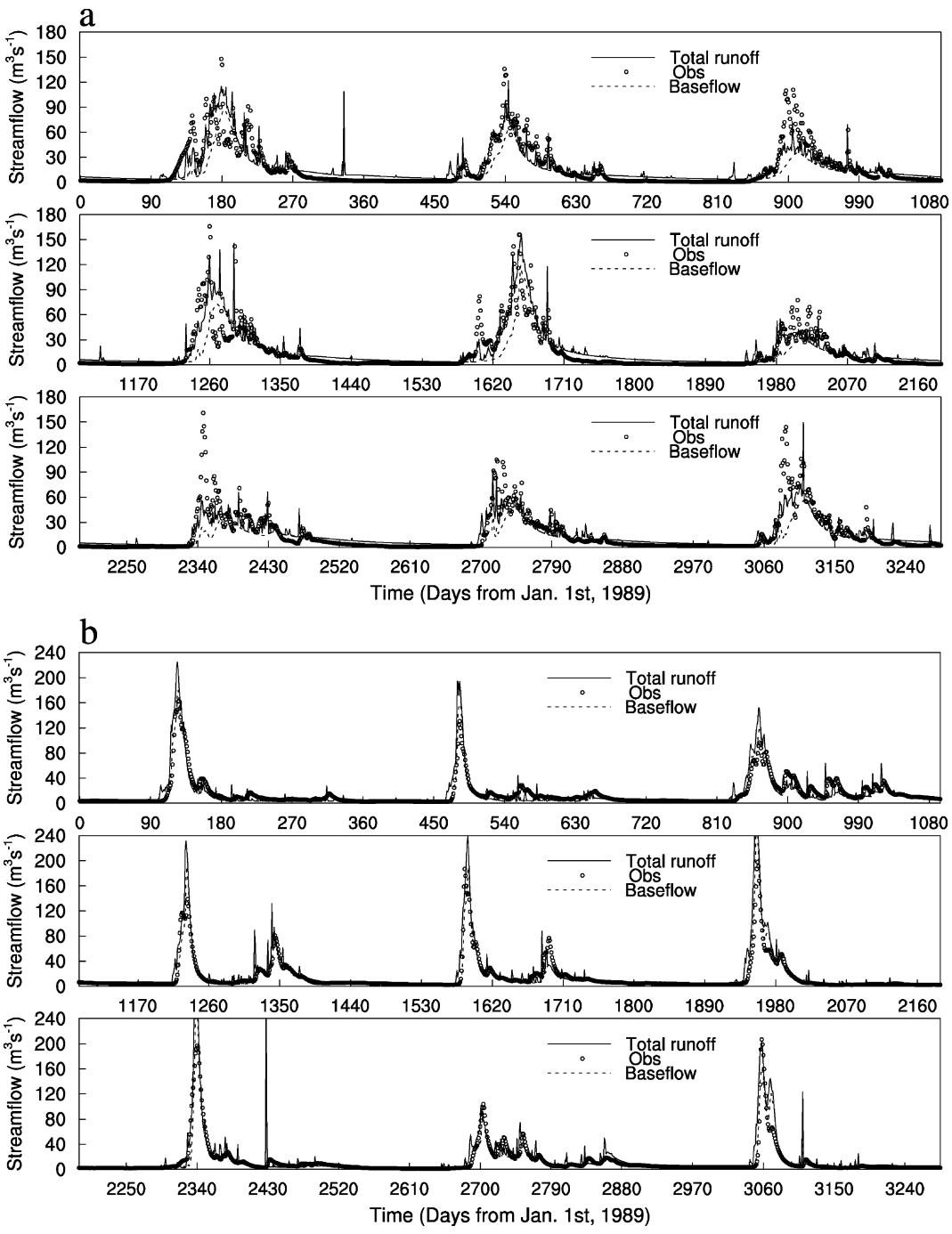

Fig. 3. (a) Time series of the modeled unrouted streamflow compared with the observed streamflow for Övre Abiskojokk. (b) Time series of the modeled unrouted streamflow compared with the observed streamflow for Övre Lansjärv.

Table 4
Surface types and the number of grid cells

Surface type code	Tile 1	Tile 2	Tile 3	Tile 4	Grid nos.
1	Close shrub	Open shrub	Bare soil	Lake	33/218
2	Wood land	Wood grass	Bare soil	Lake	150/218
3	Close shrub	Open shrub	Wood grass	Lake	31/218
4	Wood land	Wood grass	Close shrub	Lake	1/218
5	Wood land	Wood grass	Evergreen needleleaf tree	Lake	2/218
6	Grassland	Wood grass	Close shrub	Lake	1/218

The timing of peaks is different for $R_{sb,TOP}$, $R_{sb,BOT}$, and $R_{sb,SAT}$ as shown in Fig. 4. The topographic control peak has the same timing as the water table peak, which is similar to the timing of the saturation excess peak. The bottom drainage peak is much delayed because of a large time scale involved in the transport of soil water from the model surface to the bottom.

5. Sensitivity tests

Due to the uncertainties in determining f and α, we will test the model's sensitivities to these two parameters. In addition, the model's sensitivities to the lake fraction and the topographic index are also assessed.

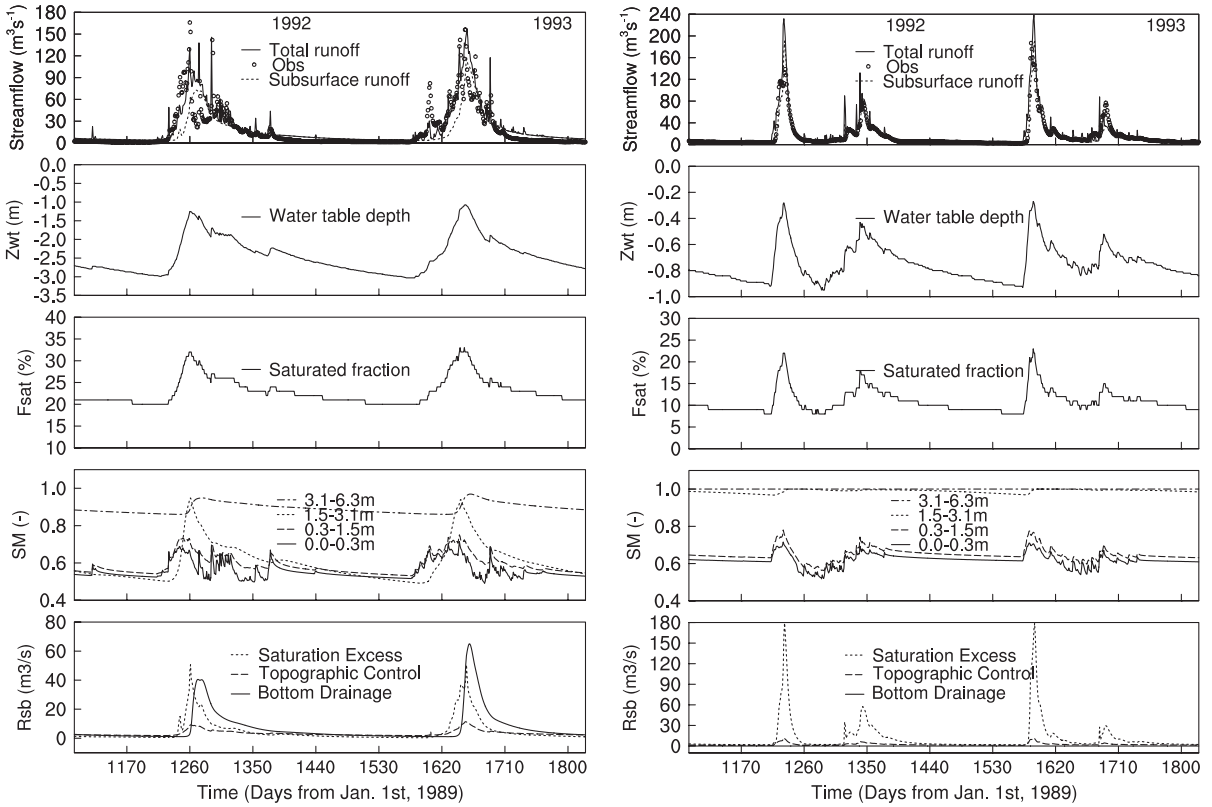

Fig. 4. Time series of the modeled unrouted streamflow, water table depth, saturated fraction, soil moisture at different layers, and subsurface runoff due to saturation excess, topographic control, and bottom drainage for Övre Abiskojokk (left panel) and Övre Lansjärv (right panel). The observed streamflow is also shown.

5.1. Sensitivity to saturated hydraulic conductivity decay factor, *f*

The decay factor, *f*, is the most important parameter in the TOPMODEL framework, because it is used in determining the vertical profile of saturated hydraulic conductivity and, hence, the vertical distribution of soil moisture, the saturated fraction, and the baseflow. It varies widely from −2.35 to 9.15 in the literature (cf. Table 1). Its precise determination requires the observed vertical distribution of the saturated hydraulic conductivity (Famiglietti et al., 1992). It is hard to measure its horizontal distribution within a catchment or a grid cell in GCMs due to extremely heterogeneous soil textures. We have performed sensitivity tests here to investigate how *f* affects the simulated recession curves and the partitioning of subsurface runoff.

The decay factor, *f*, is crucial for controling the subsurface runoff timing. Fig. 5 shows the modeled unrouted subsurface runoff for various values of *f* compared to the observed streamflow in Övre Lansjärv in 1992, a year characterized by strong snowmelt in spring and rain in fall. In the case of *f*=2, subsurface runoff suffers a severe time lag; for *f*=3, subsurface runoff is largely improved. The best fit occurs when *f*=4. The model is relatively insensitive to *f* if it is greater than 4.

The decay factor affects the calculation of the water table depth and the saturated fraction. A larger *f* leads to a faster decline of the saturated hydraulic conductivity with depth and, hence, to a smaller bottom drainage, which promotes a rise in the water table. However, the impact of increasing *f* on the saturated fraction is not straightforward. An increase in the saturated fraction is associated with an increase

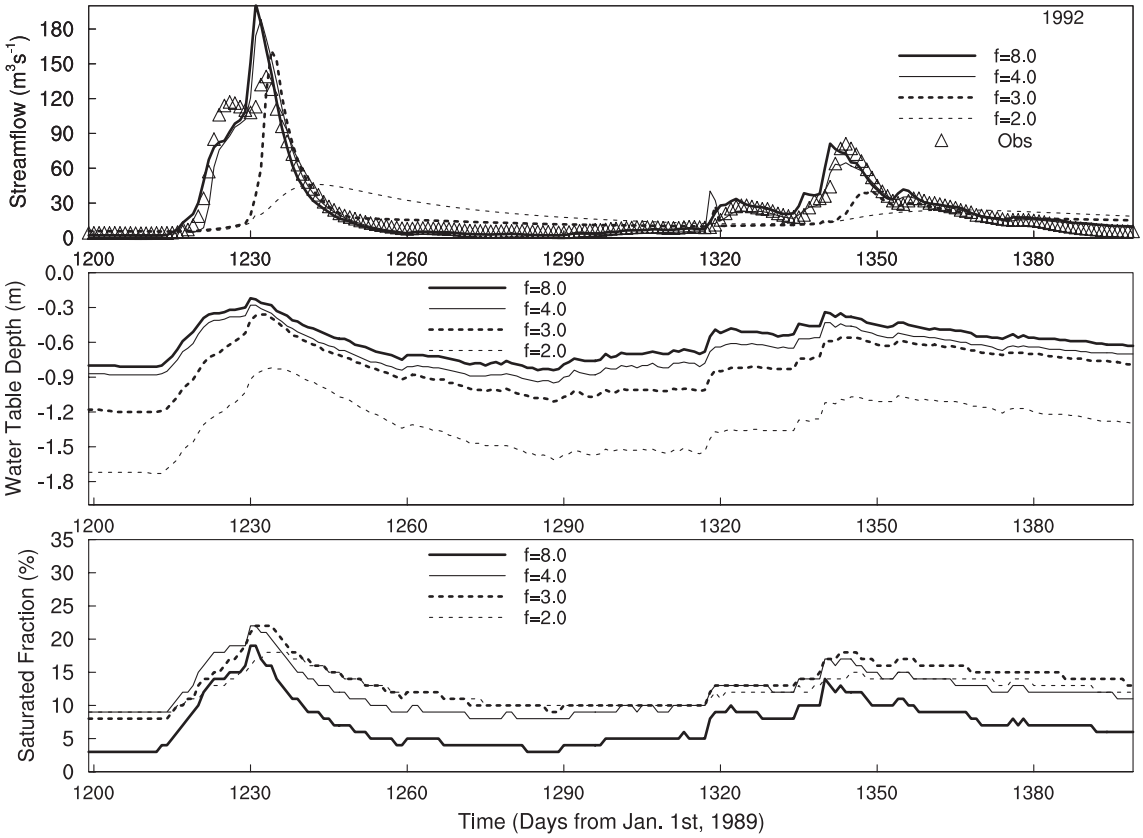

Fig. 5. Time series of the modeled unrouted subsurface runoff, water table depth, and saturated fraction for different values of *f* in Övre Lansjärv.

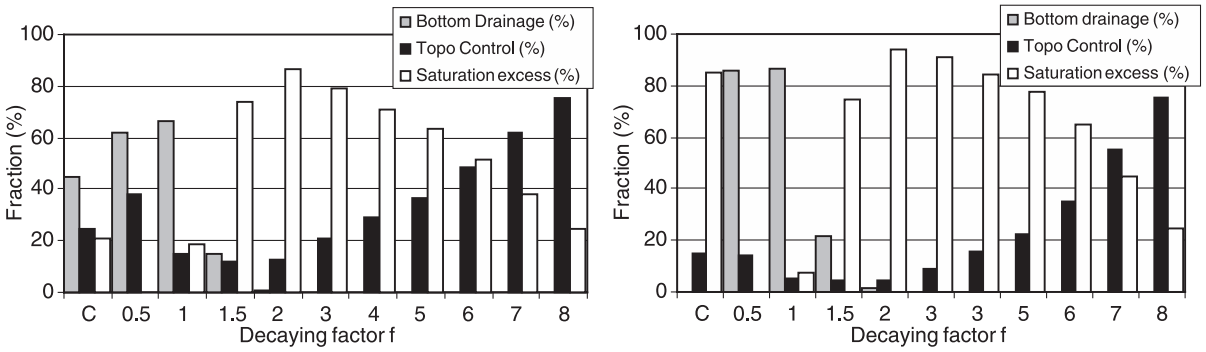

Fig. 6. Ten-year averaged fraction of subsurface runoff due to bottom drainage, topographic control, and saturation excess in Övre Abiskojokk (left) and Övre Lansjärv (right).

in f from 2 to 3, whereas the saturated fraction starts to decrease if f increases further.

The decay factor, f, is crucial in estimating $R_{sb,TOP}$. The 10-year averaged results of $R_{sb,TOP}$, $R_{sb,BOT}$, and $R_{sb,SAT}$ for various values of f are shown in Fig. 6. $R_{sb,TOP}$ increases as f increases from 2 to 8, whereas $R_{sb,SAT}$ decreases for the same range of f. $R_{sb,BOT}$ dominates if f is less than 2. For the same f value, $R_{sb,TOP}$ is always larger in Övre Abiskojokk than in Övre Lansjärv because the former has a smaller mean topographic index. Although f affects both surface and subsurface runoff compoents, total runoff is relatively not affected (Fig. 7). Notice that the Torne–Kalix basin lies above the Arctic Circle and, hence, is energy limited. How f influences total runoff in midlatitudes and in tropics will be subject to future study.

5.2. Sensitivity to anisotropic factor

The anisotropic factor was first introduced by Chen and Kumar (2001) to account for the differences in the saturated hydraulic conductivities in the lateral and the vertical directions. They used $\alpha = 2000$, meaning that the saturated hydraulic conductivity is 2000 times as large in the lateral direction as in the vertical direction. Our test showed that the soil dries out quickly if $\alpha = 2000$ is used and that $R_{sb,TOP}$ is negligible if $\alpha = 1$ is used. In the control run, $\alpha = e^{2.5} = 12.2$ was used to fit the observed recession curve.

We have done five sensitivity experiments with $\alpha = e^0$, e^1, e^2, e^3, and e^4, respectively. As α increases from e^0 to e^4, $R_{sb,TOP}$ increases from 1.37% to 46.65% in Övre Lansjärv and from 2.32% to 62.91% in Abiskojokk. However, subsurface runoff, surface run-

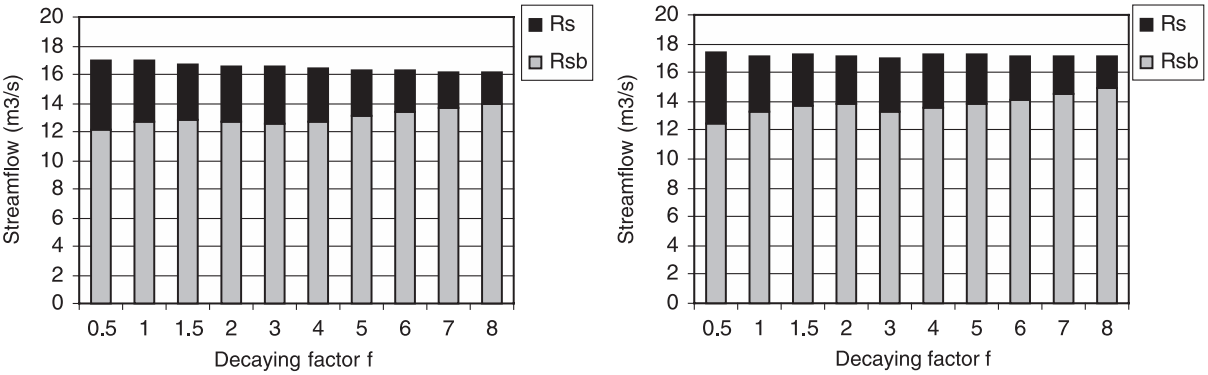

Fig. 7. Ten-year averaged modeled unrouted surface (R_s) and subsurface runoff (R_{sb}) in Övre Abiskojokk (left) and Övre Lansjärv (right).

Table 5
Sensitivities to the anisotropic factor

Subbasin	α	R (m^3/s)	R_s (m^3/s)	R_{sb} (m^3/s)	$R_{sb,BOT}$ (%)	$R_{sb,TOP}$ (%)	$R_{sb,SAT}$ (%)
Lansjärv	$e^0=1$	17.15	3.85	13.30	0.00	1.37	98.63
	$e^1=2.72$	17.15	3.83	13.32	0.00	3.65	96.35
	$e^2=7.39$	17.15	3.77	13.38	0.00	9.48	90.52
	$e^3=20.09$	17.15	3.61	13.54	0.00	22.83	77.16
	$e^4=54.60$	17.17	3.25	13.92	0.00	46.65	53.34
Abiskojokk	$e^0=1$	16.85	4.41	12.44	64.54	2.32	33.13
	$e^1=2.72$	16.85	4.39	12.46	61.07	6.19	32.73
	$e^2=7.39$	16.85	4.33	12.52	52.37	15.94	31.70
	$e^3=20.09$	16.85	4.14	12.71	34.75	36.13	29.12
	$e^4=54.60$	16.91	3.73	13.18	13.38	62.91	23.70

R = total runoff; R_s = surface runoff; R_{sb} = subsurface runoff; $R_{sb,BOT}$ = bottom drainage; $R_{sb,TOP}$ = topographic control; $R_{sb,SAT}$ = saturation excess.

off, and total runoff change little (Table 5). In our model, α cannot exceed e^5 despite $\alpha=2000$ in Chen and Kumar (2001); otherwise, the soil would dry out to below zero.

5.3. Sensitivity to lake fraction

In the 'without lake' experiment, it is assumed that the saturated fraction for the lake tile is zero; hence, runoff is zero as in the original NCAR LSM (Bonan, 1996). In addition, the water table depth for the lake tile is prescribed at the model bottom (6.3 m). Fig. 8 shows the saturated fraction and the water table depth simulated with and without lake. Both variables show systematic reduction in the 'without lake' experiment and total surface runoff decreases by 3% and 28% in Övre Lansjärv and Övre Abiskojokk, respectively.

5.4. Sensitivity to DEM resolution

Higher-resolution DEMs describes the contribution area and the local slopes more accurately. Because the topographic index computed from the 1000 m DEM is larger than that from the 100 m DEM by about 2 (cf.

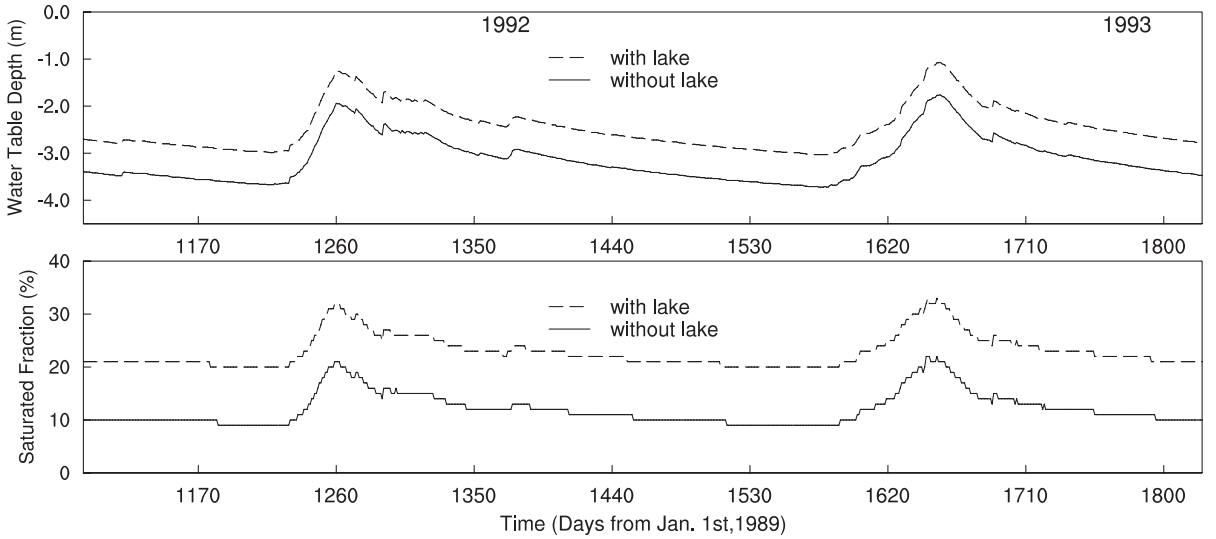

Fig. 8. Time series of the modeled water table depth and saturated fraction with/without lakes in Övre Abiskojokk.

Table 6
Sensitivities to the DEM resolution

		R (m^3/s)	R_s (m^3/s)	R_{sb} (m^3/s)	$R_{sb,BOT}$ (%)	$R_{sb,TOP}$ (%)	$R_{sb,SAT}$ (%)
Lansjärv	Ctrl	17.15	3.71	13.44	0.00	14.92	85.08
	Without Eq. (8)	17.15	4.08	13.07	0.00	1.43	98.57
Abiskojokk	Ctrl	16.85	4.26	12.59	44.64	24.67	30.69
	Without Eq. (8)	16.86	4.64	12.22	64.19	2.62	33.19

R = total runoff; R_s = surface runoff; R_{sb} = subsurface runoff; $R_{sb,BOT}$ = bottom drainage; $R_{sb,TOP}$ = topographic control; $R_{sb,SAT}$ = saturation excess.

Eq. (8)), $R_{sb,TOP}$ from using the 1000 m DEM is smaller by a factor of e^2 compared to that from using the 100 m DEM. If the topographic index from the 1000 m DEM is employed without adjustment by Eq. (8), $R_{sb,TOP}/R_{sb}$ is decreased from 14.92% to 1.43% in Övre Lansjärv and from 24.67% to 2.62% in Abiskojokk (Table 6).

6. An alternative scheme of subsurface runoff (VISA-TOP2)

We seek an alternative parameterization of the production of subsurface runoff due to saturation excess, $R_{sb,SAT}$. In this framework, the soil column saturation excess is first used to recharge the soil

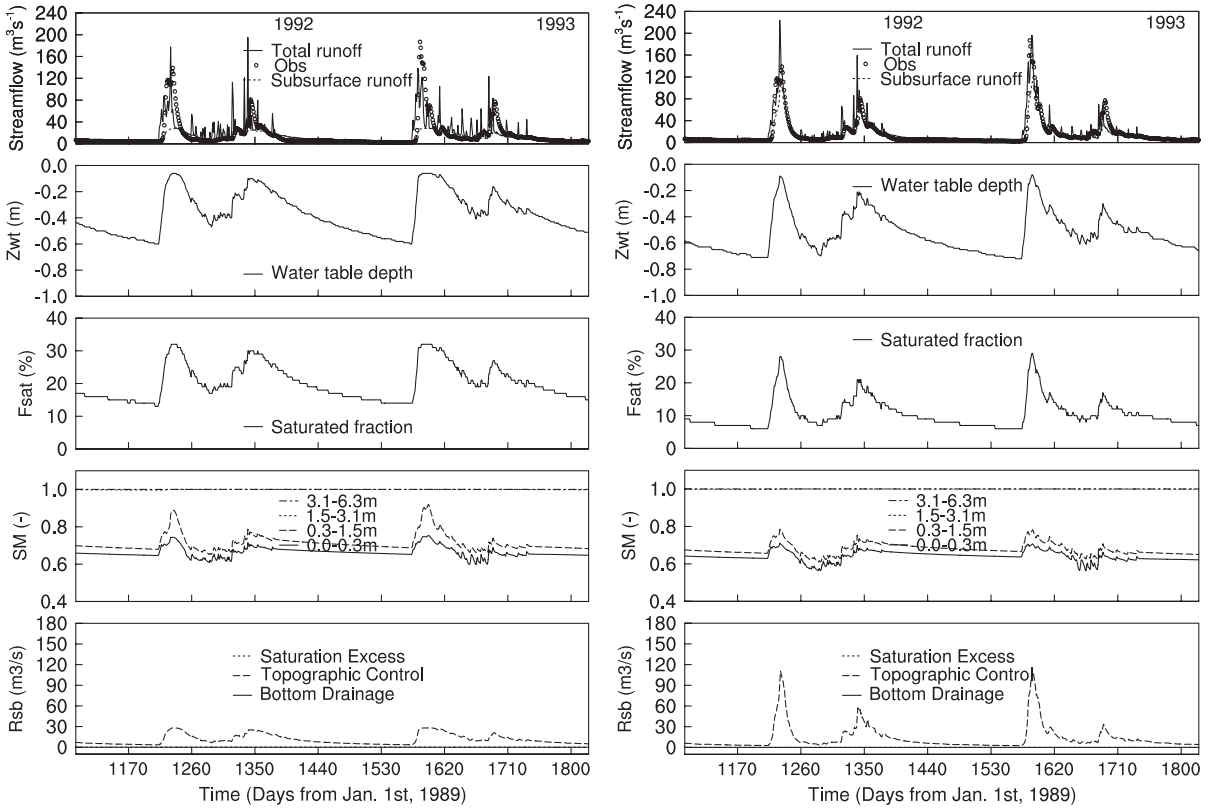

Fig. 9. Time series of the modeled unrouted total runoff compared with the observed streamflow, water table depth, saturated fraction, soil moisture, and subsurface runoff components due to saturation excess, topographic control, and bottom drainage for $f = 4$ (left) and $f = 6$ (right) in Övre Lansjärv using VISA-TOP2.

layers above the water table, while the formulations of $R_{sb,TOP}$ and $R_{sb,BOT}$ remain the same as in VISA-TOP1. In this case, $R_{sb,SAT}$ can still be greater than zero if the entire soil column is oversaturated. The resulting version is called VISA-TOP2.

Fig. 9 (left panel) shows the simulations from VISA-TOP2 in direct comparison with those in Fig. 4 (right panel) from VISA-TOP1. The chief difference in the two experiments is how the saturation excess is handled. With the saturation excess water recharged back to the soil layers above the water table in VISA-TOP2, the water table depth becomes shallower than that in VISA-TOP1 as expected. The saturated fraction in VISA-TOP2 almost reaches its maximum value during the intensive recharging period. Although surface runoff increases, it is too small to compensate the decrease in subsurface runoff. Therefore, VISA-TOP2 fails to capture the observed recession curve. If the decay factor increases to $f=6$, subsurface runoff is largely increased (Fig. 9, right panel). The soil moisture decreases and the water table falls. Judging from the simulations of streamflow, VISA-TOP2 has the best fit with $f=6$, while VISA-TOP1 uses $f=4$. This indicates that different model formulations possess different values of optimum parameters.

Like VISA-TOP1, VISA-TOP2 is strongly sensitive to f. The detailed patterns are, however, dramatically different. In VISA-TOP2, the water table is confined to near the surface and the saturated fraction spreads between 0 and 35%. As f increases, the water table falls due to increased subsurface runoff. The saturated fraction also decreases as the water table depth increases. In the case of $f=2$, almost the entire

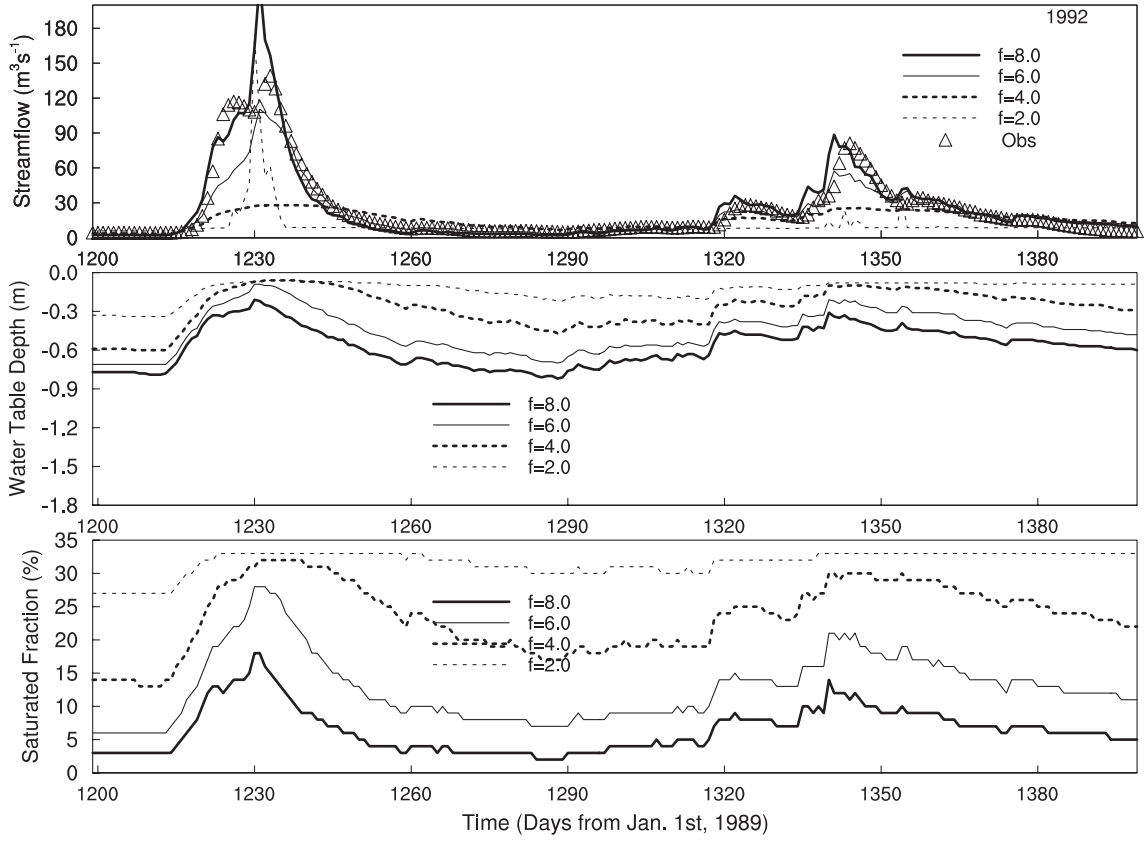

Fig. 10. Time series of the modeled unrouted subsurface runoff compared with the observed streamflow, water table depth, saturated fraction for different values of f in Övre Lansjärv using VISA-TOP2.

soil column is oversaturated during the late spring when snowmelt reaches its peak (around day 1230 in Fig. 10), and the oversaturated water runs off directly.

We have also tested the model's sensitivity to the anisotropic factor α in the case of $f=6$, for various values of $\alpha=e^x$, where $x=1, 2, 3, 4$. The simulations of unrouted subsurface runoff, water table depth, and saturated fraction are strongly sensitive to α. Increasing its value directly increases subsurface runoff, lowers the water table, and reduces the saturated fraction (Fig. 11). If x is less than 2, VISA-TOP2 fails to capture the observed recession curve. The case $x=0$ (not shown) corresponds to the original TOPMODEL formulations, but it is unable to obtain the observed recession curve, indicating this factor is necessary in VISA-TOP2. The anisotropic factor may be interpreted here to compensate the error due to use of coarse resolution DEMs. Although the topographic index from the 1000 m DEM has been adjusted using the 100 m DEM (cf. Eq. (8)), this adjustment alone may not be adequate. Indeed, Eq. (8) was derived based on the 100 and 1000 m DEMs for 50 locations in the conterminous USA (Wolock and McCabe, 2000). It is likely that this equation may need further adjustment in the Torne–Kalix basin and that this further adjustment may be accounted for by introducing the anisotropic factor.

7. Evaluation of an intermediate version (VISA-TOP3)—without topographic index

In light of the above difficulties in producing an accurate estimate of the topographic index for the

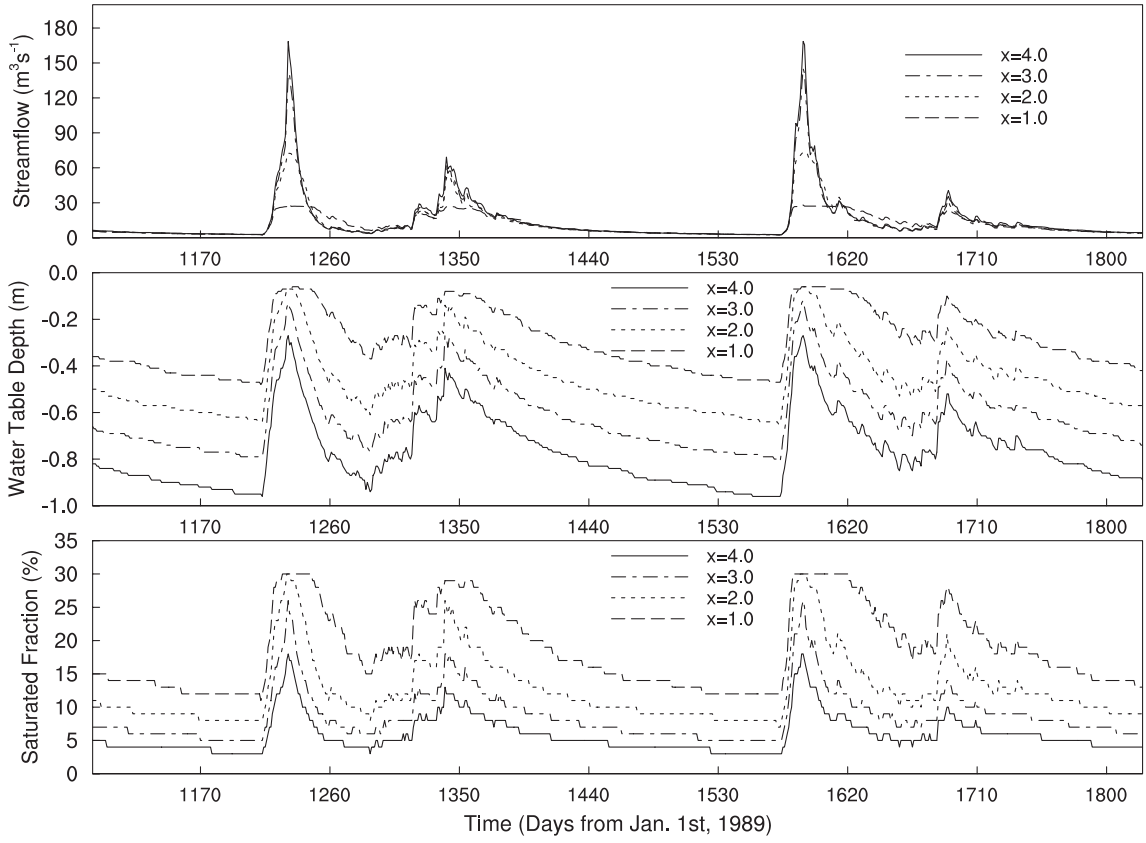

Fig. 11. Time series of the modeled unrouted subsurface runoff, water table depth, saturated fraction for different values of the anisotropic factor (x represents the power of $\alpha=e^x$) in Övre Lansjärv using VISA-TOP2.

global continents, it is attractive to develop a topography-related runoff parameterization which does not require the topographic index data set. In the simplest case, the topographic characteristics may be parameterized as constants for all land points, and the saturated fraction and subsurface runoffs are only determined by the soil moisture represented by the water table depth. The resulting version is called VISA-TOP3.

Surface runoff still takes the form of Eq. (2), but the saturated fraction is parameterized as

$$F_{\mathrm{sat}} = F_{\max} e^{-f z_{\nabla}} \tag{10}$$

where $F_{\max}$ and z_{∇} are the maximum saturated fraction and the mean water table depth of a grid cell. $F_{\max}$, corresponding to the cumulative distribution function of the topographic index when the water table depth is zero, is estimated here as 0.35 from Fig. 2.

Subsurface runoff due to the topographic control is parameterized as

$$R_{\mathrm{sb,TOP}} = R_{\mathrm{sb,max}} e^{-f z_{\nabla}} \tag{11}$$

where $R_{\mathrm{sb,max}}$ is the maximum subsurface runoff and $R_{\mathrm{sb,max}} = 1.0 \times 10^{-4}$ (mm/s) = 8.64 (mm/day). The other components of subsurface are the same as in VISA-TOP2.

Using $f = 2$ for Övre Abiskojokk and $f = 6$ for Övre Lansjärv, VISA-TOP3 also reproduces the observed streamflow (Fig. 12). Although the simulations of total runoff, water table depth, soil moisture, and subsurface runoff are similar to those from VISA-TOP2, the saturated fraction is much smaller than that from VISA-TOP2 (cf. Figs. 9 and 12), indicating that

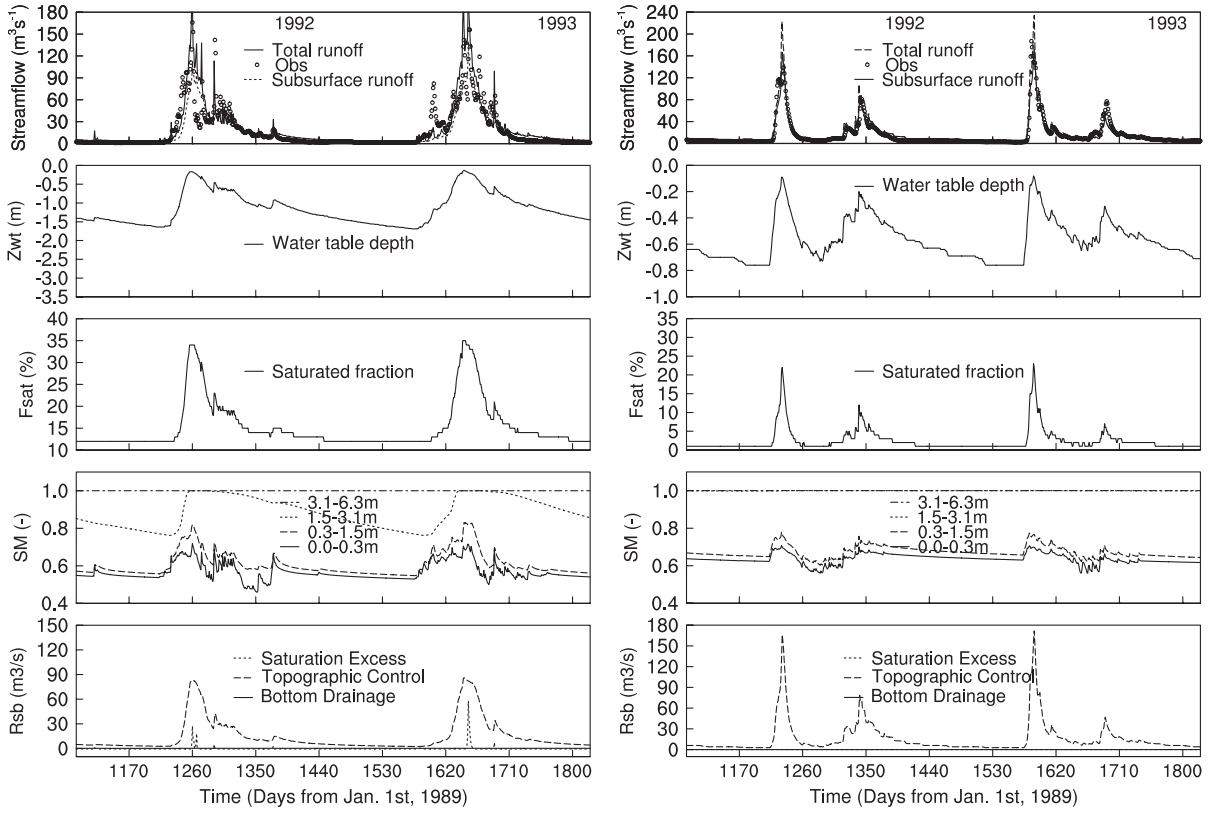

Fig. 12. Time series of the modeled unrouted streamflow compared with the observed streamflow, water table depth, saturated fraction, soil moisture at different layers, and subsurface runoff components due to saturation excess, topographic control, and bottom drainage for Övre Abiskojokk (left) and Övre Lansjärv (right) using VISA-TOP3.

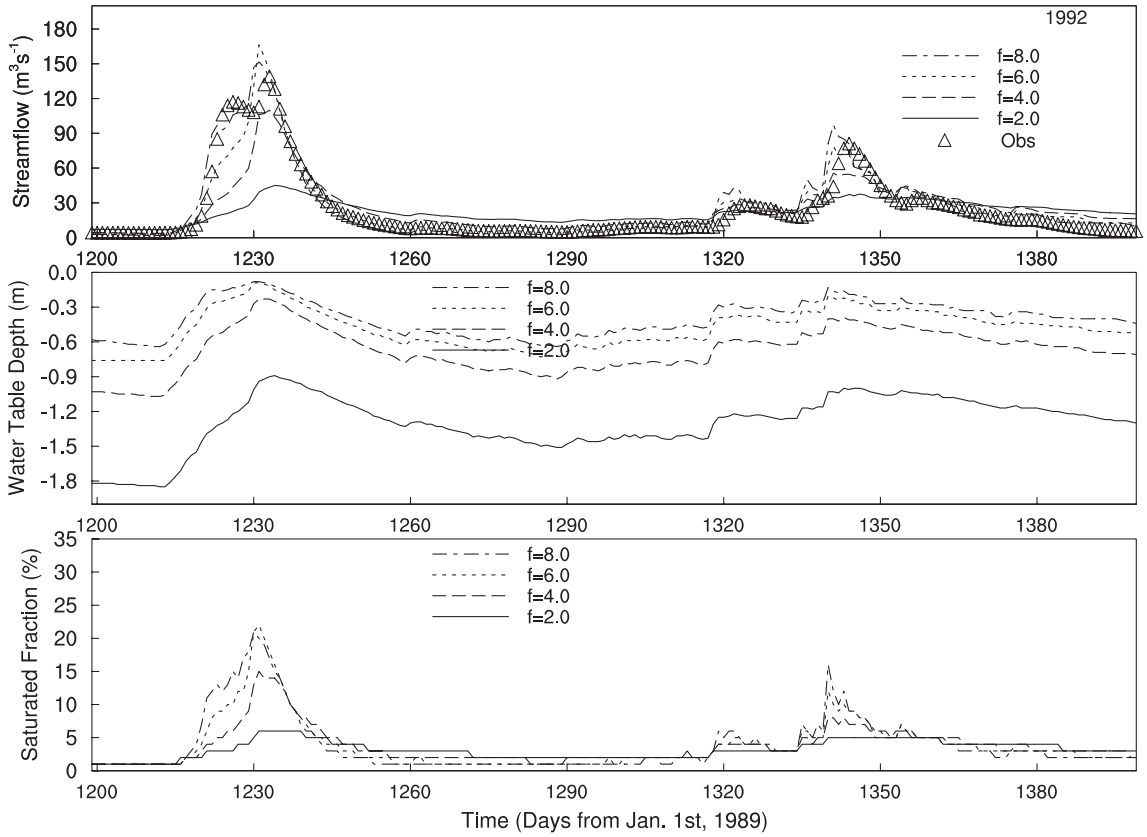

Fig. 13. Time series of the modeled unrouted subsurface runoff compared with the observed streamflow, water table depth, saturated fraction for different values of f using VISA-TOP3.

the simulated surface runoff is different between these two schemes. Like VISA-TOP2, VISA-TOP3 is sensitive to f (cf. Figs. 10 and 13). However, the patterns in the simulations of water table depth and saturated fraction are dramatically different, suggesting that f plays different roles in different model formulations.

8. Summary and conclusion

Three topography-based runoff schemes in VISA have been evaluated using the data set for Övre Lansjärv and Övre Abiskojokk. VISA-TOP1 differs from VISA-TOP2 only in how to treat saturation excess or oversaturated soil water from the soil layers. In VISA-TOP1, the oversaturated soil water is thrown out of the soil column; hence, it no longer plays a role in the ensuing soil water budgets. In VISA-TOP2, this oversaturated soil water is recharged back to the unsaturated soil layers above the water table; hence, it continues to involve in the water budgets. Unlike VISA-TOP1 and VISA-TOP2, VISA-TOP3 relaxes its dependence on the topographic parameters. Using a global mean constant of the topographic index, F_{sat} and $R_{sb,TOP}$ are only dependent on the water table depth and the saturated hydraulic conductivity decay factor. The oversaturated soil water is treated the same in both VISA-TOP2 and VISA-TOP3.

The intercomparison of the modeled unrouted runoff with the observed streamflow reveals that VISA-TOP1 reproduces the daily and seasonal variations of streamflow. Sensitivity tests indicate that the simulations of runoff, water table depth, and saturated fraction are strongly sensitive to the saturated hydraulic conductivity decay factor, the anisotropic factor, lake fractions, and the topographic index

modification due to DEM resolutions. The decay factor, f, controls the timing and partitioning of subsurface runoff. The anisotropic factor is necessary for the successful implementation of TOPMODEL into SVATs. The topographic index computed from coarser resolution DEMs need to be adjusted using available finer resolution DEMs. The regression equation proposed by Wolock and McCabe (2000) improved the simulations of the topography-controled subsurface runoff.

In the VISA-TOP2 scheme, the topography-controled subsurface runoff is dominant because the oversaturated water is recharged to upper unsaturated soil layers to raise the water table. VISA-TOP2 reproduces the simulations from VISA-TOP1 provided that different values of f are used in both schemes. The water table depth and the saturated fraction in VISA-TOP1 and VISA-TOP2 show dramatically different responses to changes in f. Relaxing the dependence on the topographic parameters, VISA-TOP3 also is capable of reproducing the observed streamflow provided that f is adjusted.

In this study, f and α are identified as two adjustable parameters. Both have physical meanings at local scales. In a catchment or a GCM grid cell, however, both parameters are quasi-physical and need to be calibrated against observations due to large subgrid heterogeneity of surface conditions. The anisotropic factor is a parameter which was first introduced by Chen and Kumar (2001) merely to produce the desired streamflow. It may be interpreted as a compensating agent to reduce the error caused from using a coarse-resolution DEM in calculating the topographic index. The calibrated values of f are different in VISA-TOP1, VISA-TOP2 and VISA-TOP3, indicating that the calibrated parameters and the model formulations should not be separated. Such issue has been discussed by Beven (1997) in terms of the model equifinality. Additional research is required to evaluate these formulations and parameters on continental and global scales.

Acknowledgements

The comments from two anonymous reviewers lead to improvement of this paper. The authors would like to thank Dr. Wolock for providing us the GIS ARC/INFO program to compute the topographic index, and Laura Bowling and Dr. Dennis Lettenmaier for making the PILPS 2e data available. Dr. Robert E. Dickinson is thanked for his original idea in using global mean topographic parameters in the common land model, and this idea prompts us to formulate VISA-TOP3. This work was funded by NASA grant NAG8-1520 and NSF grant ATM0095094.

References

Beven, K.J., 1982. On subsurface stromflow: an analysis of response times. Hydrol. Sci. J. 27, 505–521.

Beven, K.J., 1997. TOPMODEL: a critique. Hydrol. Process. 11 (9), 1069–1085.

Beven, K.J., Kirkby, M.J., 1979. A physically based, variable contributing model of basin hydrology. Hydrol. Sci. Bull. 24, 43–69.

Beven, K.J., Quinn, P., Romanowicz, R., Freer, J., Fisher, J., Lamb, R., 1994. TOPMODEL and GRIDATB, a Users Guide to the Distribution Versions (94.01). Tech Rep. TR110/94. Centr. For Res. on Environ. Syst. and Stat., Lancaster University, Lancaster, U.K.

Beven, K.J., Lamb, R., Quinn, P.F., Romanowicz, R., Freer, J., 1995. TOPMODEL. In: Singh, V.P. (Ed.), Computer Models of Watershed Hydrology. Water Resour. Publ., Highlands Ranch, CO, pp. 627–668.

Bonan, G.B., 1996. A land surface model (LSM version 1.0) for ecological, hydrological, and atmospheric studies: technical description and user's guide. NCAR Technical Note NCAR/TN-417+STR. National Center for Atmospheric Research, Boulder, CO. 150 pp.

Bowling, L.C., Lettenmaier, D.P., Nijssen, B., Graham, L.P., Clark, D.B., Maayar, M.E., Essery, R., Goers, S., Gusev, Y.M., Habets, F., Hurk, B.V.D., Jin, J., Kahanl, D., Lohmann, D., Ma, X., Mahanamao, S., Mocko, D., Nasonova, O., Niu, G.-Y., Samuelsson, P., Shmakin, A.B., Takata, K., Verseghy, D., Viterbo, P., Xia, Y., Xue, Y., Yang, Z.-L., 2003. Simulation of high latitude hydrological processes in the Torne–Kalix basin: PILPS Phase 2(e) 1: experiment description and summary intercomparisons. Glob. Planet. Change 38, 1–30.

Chen, J., Kumar, P., 2001. Topographic influence on the seasonal and inter-annual variation of water and energy balance of basins in North America. J. Climate 14, 1989–2014.

Clapp, R.B., Hornberger, G.M., 1978. Empirical equations for some soil hydraulic properties. Water Resour. Res. 14, 601–604.

Dai, Y., Zeng, X., Dickinson, R.E., Baker, I., Bonan, G., Bosilovich, M., Denning, S., Dirmeyer, P., Houser, P., Niu, G.-Y., Oleson, K., Schlosser, A., Yang, Z.-L., 2003. The Common Land Model (CLM). Bull. Am. Meteor. Soc. (in press).

Dickinson, R.E., Shaikh, M., Bryant, R., Graumlich, L., 1998. Interactive canopies for a climate model. J. Climate 11, 2823–2836.

Ducharne, A., Koster, R.D., Suarez, M.J., Stieglitz, M., Kumar, P.,

2000. A catchment-based approach to modeling land surface processes in a general circulation model: 2. Parameter estimation and model demonstration. J. Geophys. Res. 105 (D20), 24823–24838.

Entekhabi, D., Eagleson, P.S., 1989. Land surface hydrology parameterization for atmospheric general circulation models including subgrid-scale spatial variability. J. Climate 2, 816–831.

Famiglietti, J.S., Wood, E.F., 1991. Evapotranspiration and runoff from large land areas: land surface hydrology for atmospheric general circulation models. Surv. Geophys. 12, 179–204.

Famiglietti, J.S., Wood, E.F., Sivapalan, M., Thongs, D.J., 1992. A catchment scale water balance model for FIFE. J. Geophys. Res. 97, 18997–19007.

Koster, R.D., Suarez, M.J., Ducharne, A., Stieglitz, M., Kumar, P., 2000. A catchment-based approach to modeling land surface processes in a general circulation model: 1. Model structure. J. Geophys. Res. 105 (D20), 24809–24822.

Sivapalan, M., Beven, K., Wood, E.F., 1987. On hydrologic similarity: 2. A scaled model of storm runoff production. Water Resour. Res. 23, 2266–2278.

Stieglitz, M., Rind, D., Famiglietti, J., Rosenzweig, C., 1997. An efficient approach to modeling the topographic control of surface hydrology for regional and global modeling. J. Climate 10, 118–137.

Wolock, D.M., McCabe, G.J., 2000. Differences in topographic characteristics computed from 100- and 1000-m resolution digital elevation model data. Hydrol. Process. 14, 987–1002.

Yang, Z.-L., Niu, G.-Y., 2003. The Versatile Integrator of Surface Atmospheric Processes (VISA): Part 1. model description. Submitted to Global Planet. Change 38, 175–189.

Yang, Z.-L., Niu, G.-Y., Dickinson, R.E., Stieglitz, M., 2000. Parameterization of runoff production in common land model. EOS Trans. AGU, Spring Meet., Suppl. 81 (19), S139.